

Supplementary information to accompany:

4,2':6',4''- and 3,2':6',3''-terpyridines: the conflict between well-defined vectorial properties and serendipity in the assembly of 1D-, 2D- and 3D- architectures

Y. Maximilian Klein^a, Alessandro Prescimone^a, Edwin C. Constable^a and Catherine E. Housecroft^{*a}

^aDepartment of Chemistry, University of Basel, Spitalstrasse 51, 4056 Basel, Switzerland.

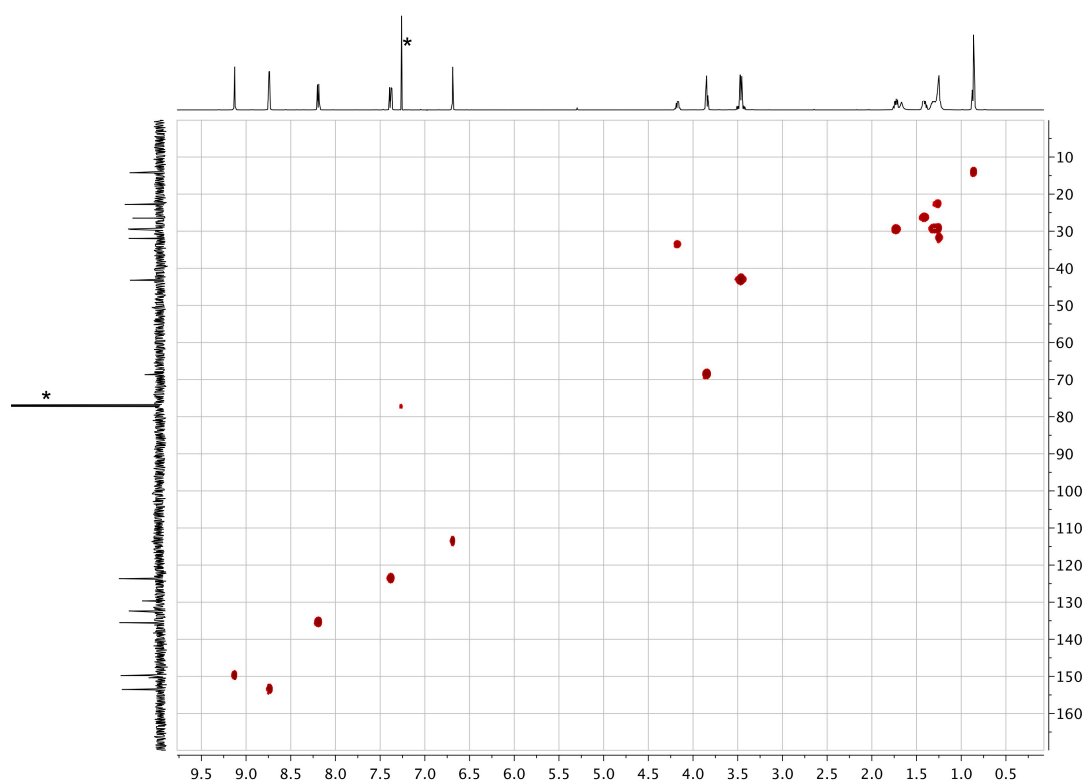


Fig. S1. HMQC (500 MHz ¹H NMR and 126 MHz ¹³C NMR) spectrum of compound **9** in CDCl₃. * = residual CHCl₃.

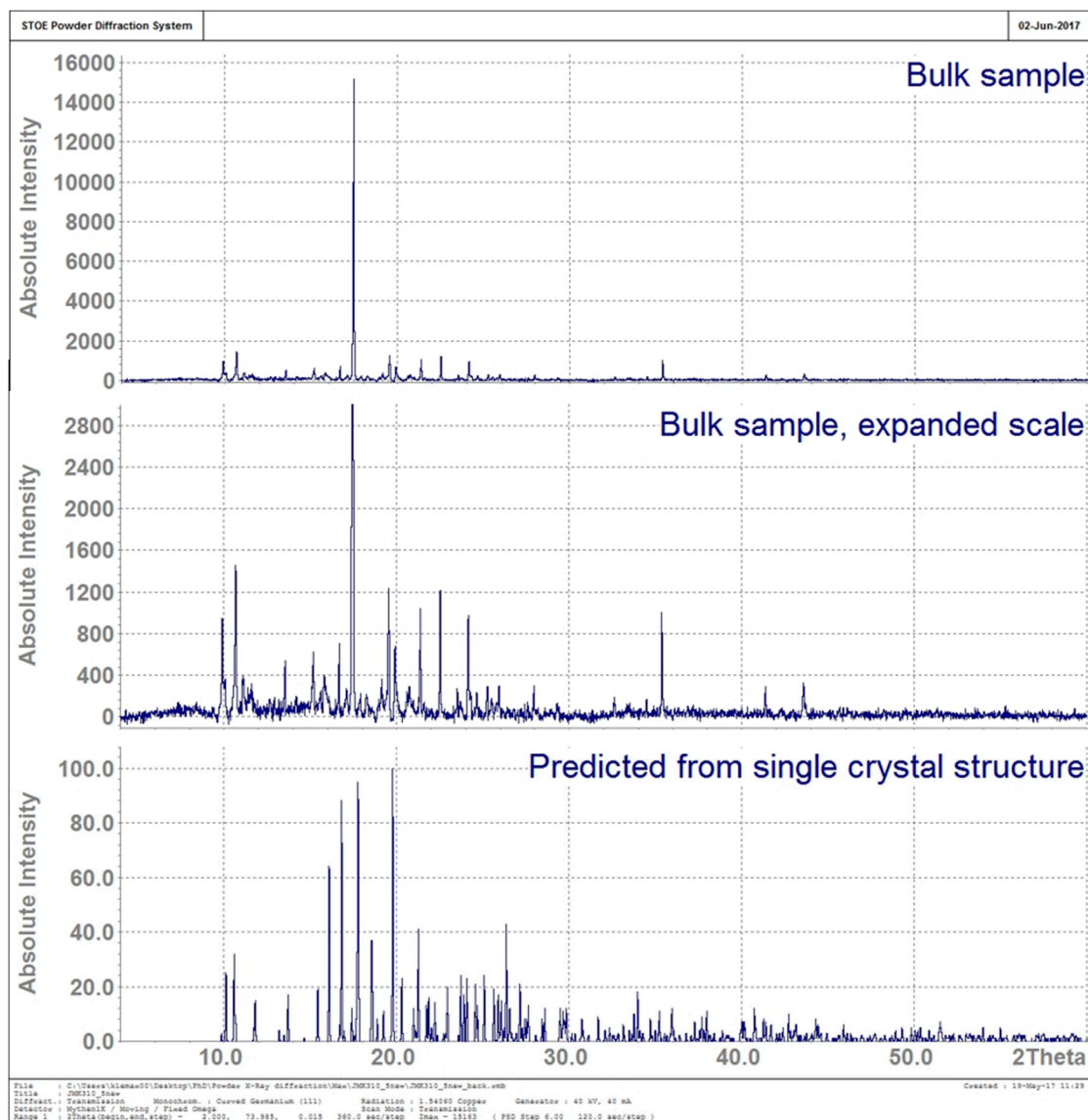


Fig. S2. Comparison of the powder diffraction patterns of the bulk sample obtained from the reaction of $\text{Co}(\text{NCS})_2$ and **7** (top two patterns, room temperature) and that predicted from the single crystal structure of $\{[\text{Co}(\text{NCS})_2(\mathbf{7})_2] \cdot 4\text{CHCl}_3\}_n$ (123 K). Differences between the peak intensities of the measured bulk samples compared to predicted patterns most likely arise from preferred orientations of the crystals in the bulk material. Grinding the sample more did not change the relative peak intensities but signal-to-noise ratios decreased dramatically.

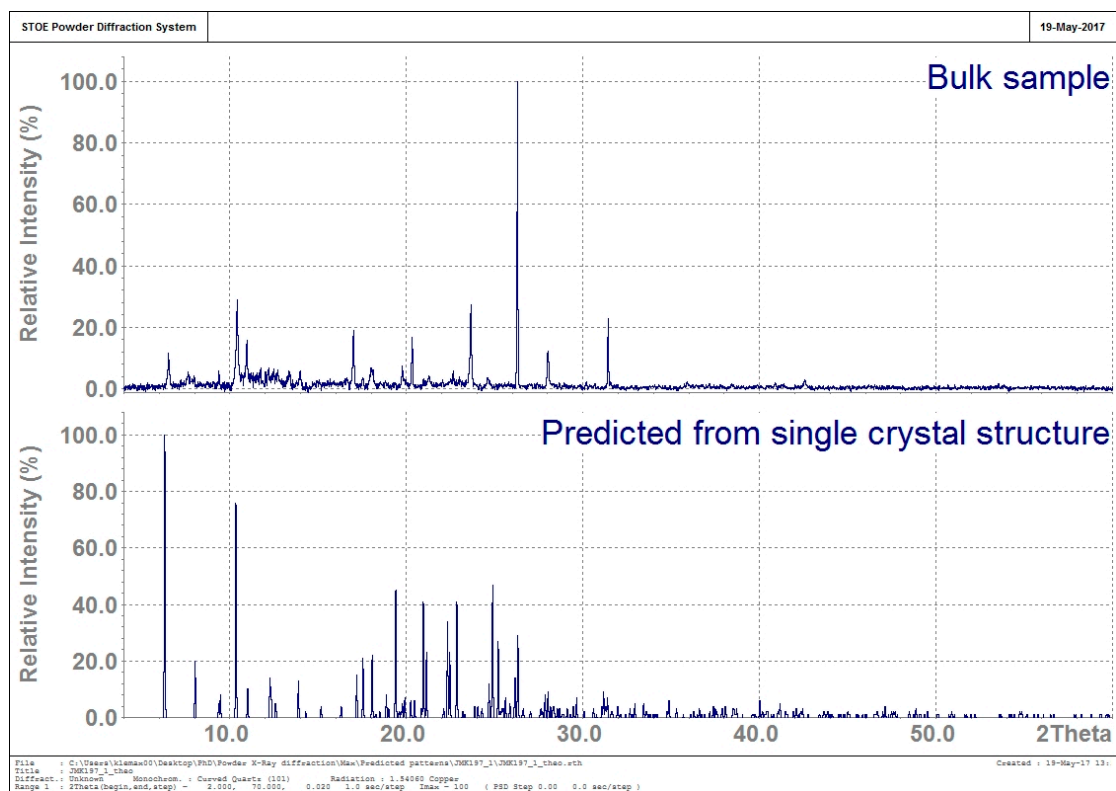


Fig. S3. Comparison of the powder diffraction patterns of the bulk sample obtained from the reaction of $\text{Co}(\text{NCS})_2$ and **8** (top, room temperature) and that predicted from the single crystal structure of $\{[\text{Co}(\text{NCS})_2(\mathbf{8})_2] \cdot 2\text{C}_6\text{H}_4\text{Cl}_2\}_n$ (123 K).

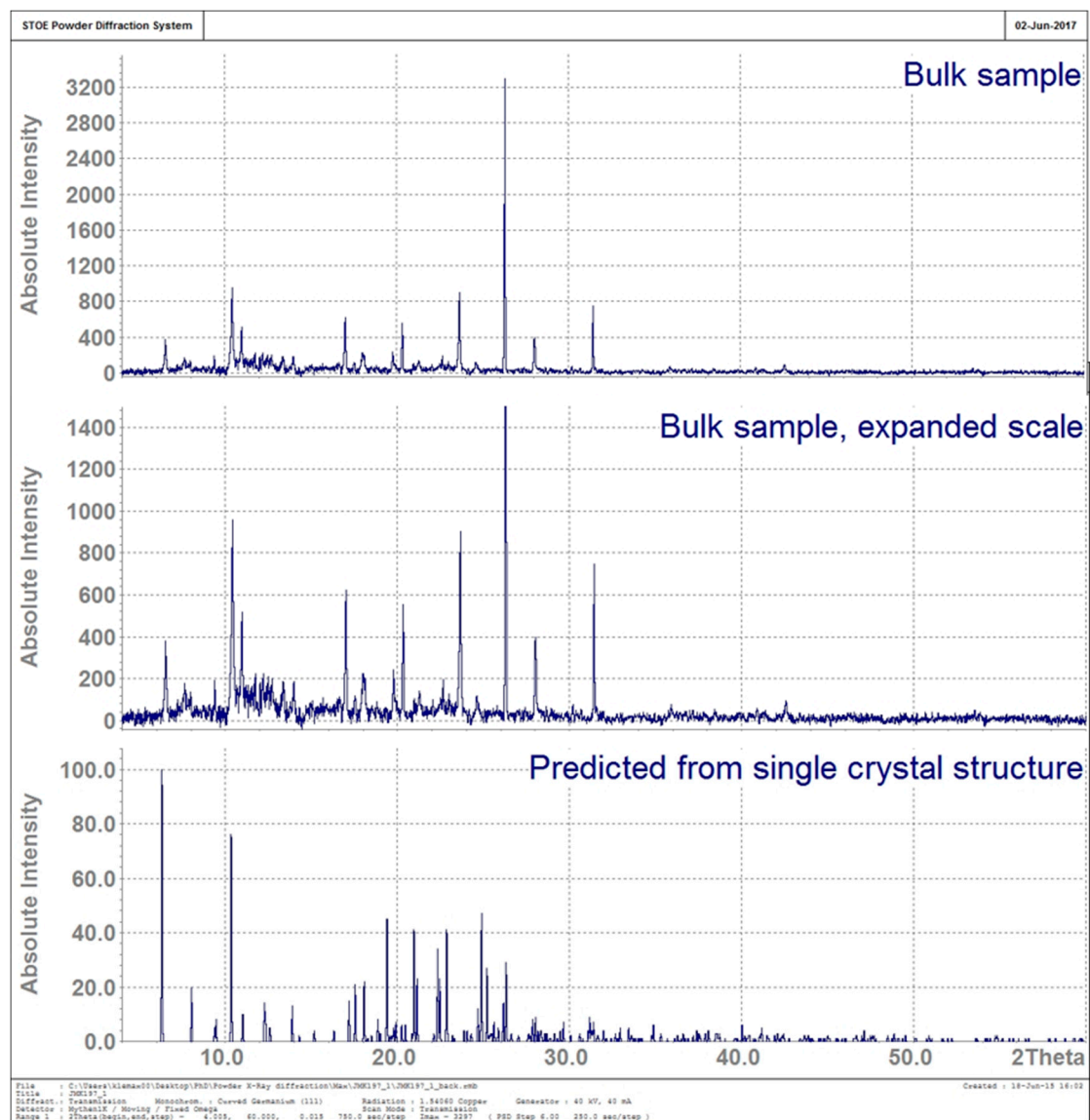


Fig. S4. Comparison of the powder diffraction patterns of the bulk sample obtained from the reaction of $\text{Co}(\text{NCS})_2$ and **9** (top, room temperature) and that predicted from the single crystal structure of $\{[\text{Co}(\text{NCS})_2(\mathbf{9})] \cdot 2\text{CHCl}_3\}_n$ (123 K). Differences between the peak intensities of the measured bulk samples compared to predicted patterns most likely arise from preferred orientations of the crystals in the bulk material. Grinding the sample more did not change the relative peak intensities but signal-to-noise ratios decreased dramatically.

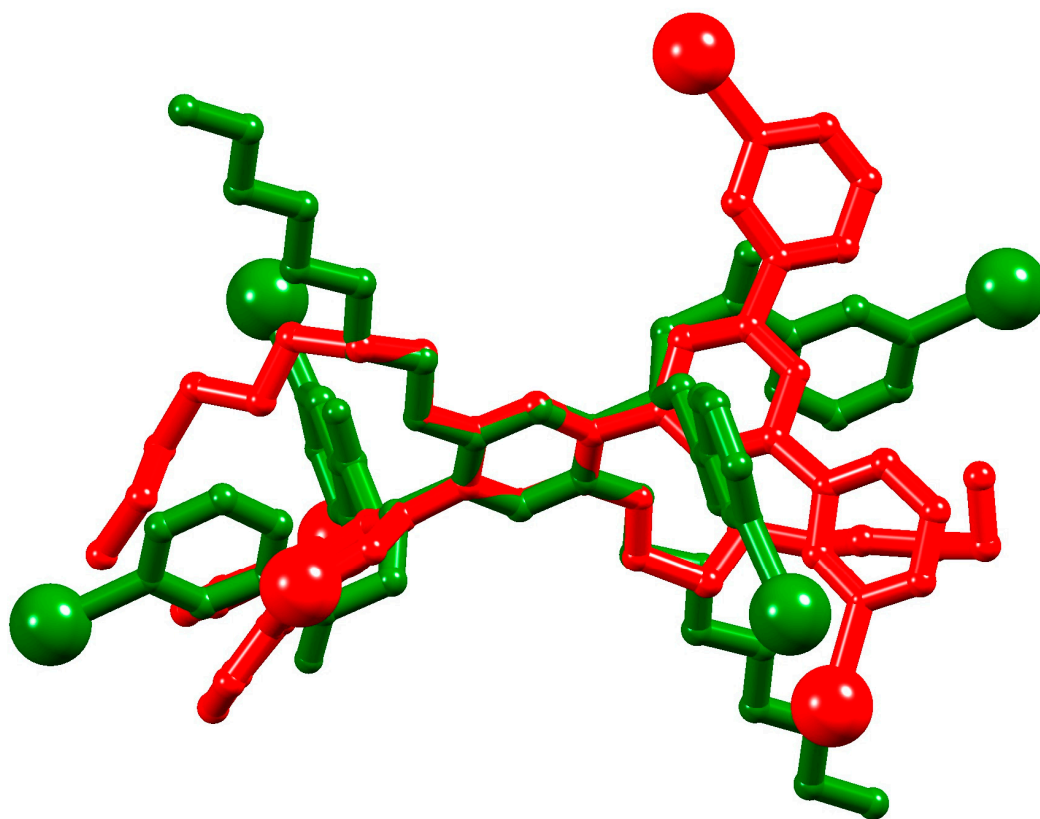


Fig. S5. Comparison of the conformations of the coordinated ligands **3** (red) and **9** (green) in $\{[\text{Co}(\text{NCS})_2(\mathbf{3})] \cdot 4\text{CHCl}_3\}_n$ and $\{[\text{Co}(\text{NCS})_2(\mathbf{9})] \cdot 2\text{CHCl}_3\}_n$, respectively. The central arene rings have been overlaid. Cobalt atoms are shown as large spheres. Ligand **3** acts as an approximately tetrahedral 4-connecting node, and **9** as a planar 4-connecting node.